A SU-8 liquid cell for surface acoustic wave biosensors

L. A. Francis[a,b], J.-M. Friedt[c], C. Bartic[b] and A. Campitelli[b]

[a] PCPM, Université catholique de Louvain, Croix du Sud 1, B-1348 Louvain-la-Neuve, Belgium;
[b] Biosensors Group, IMEC, Kapeldreef 75, B-3001 Leuven, Belgium;
[c] LMN, Université de Franche-Comté, La Bouloie, 25030 Besançon, France

ABSTRACT

One significant challenge facing biosensor development is packaging. For surface acoustic wave based biosensors, packaging influences the general sensing performance. The acoustic wave is generated and received thanks to interdigital transducers and the separation between the transducers defines the sensing area. Liquids used in biosensing experiments lead to an attenuation of the acoustic signal while in contact with the transducers. We have developed a liquid cell based on photodefinable epoxy SU-8 that prevents the presence of liquid on the transducers, has a small disturbance effect on the propagation of the acoustic wave, does not interfere with the biochemical sensing event, and leads to an integrated sensor system with reproducible properties. The liquid cell is achieved in two steps. In a first step, the SU-8 is precisely patterned around the transducers to define 120 μm thick walls. In a second step and after the dicing of the sensors, a glass capping is placed manually and glued on top of the SU-8 walls. This design approach is an improvement compared to the more classical solution consisting of a pre-molded cell that must be pressed against the device in order to avoid leaks, with negative consequences on the reproducibility of the experimental results. We demonstrate the effectiveness of our approach by protein adsorption monitoring. The packaging materials do not interfere with the biomolecules and have a high chemical resistance. For future developments, wafer level bonding of the quartz capping onto the SU-8 walls is envisioned.

Keywords: surface acoustic wave, biosensor, liquid cell, SU-8, packaging, protein, fibrinogen

1. INTRODUCTION

Initially developed for filters and delay lines in the telecommunication field, surface acoustic wave (SAW) devices have also attracted a growing interest in the sensor field.[1] The sensing principle is based on the perturbation of an elastic field propagating along the surface of a planar substrate. When the SAW is shear polarized, like SH-SAW and Love-mode sensors, the acoustic energy loss is low if a liquid is present on the surface.[2,3] These sensors are adequate as biosensors where the perturbation is caused by the adsorption of biomolecules present in solution.[4,5] The biochemical recognition results in a SAW velocity change that is monitored in real-time as an electrical delay phase through the transducers. The transduction is obtained on piezoelectric substrates thanks to interdigital transducers[6] (IDTs) that consist in a set of interdigitated electrodes with alternative electrical polarity. The separation between the IDTs defines the sensing area as sketched in Figure 1.

The transfer function of the device, which relates the amplitude of an AC electrical signal at the output transducer to its value at the input transducer, is affected when a liquid with a high dielectric permittivity value is partly or fully contacting the transducers.[7] As example, Figure 2 shows the effect of deionized water in contact with any of the transducers on a quartz substrate. The attenuation observed in the amplitude and the phase of the transfer function is mainly due to an extra capacitance loading of the transducers; more details related to this effect are given in Appendix A. The intensity of the attenuation is function of the value of the electromechanical coupling constant K^2 of the piezoelectric substrate. It is more intense for low K^2 substrates such as quartz than for high K^2 substrates such as lithium niobate or lithium tantalate. For Love-mode sensors, it also depends of the thickness of the guiding dielectric overlayer that acts as shielding and reduces the interaction with liquids.

Further author information:
L. A. Francis: E-mail: francis@pcpm.ucl.ac.be

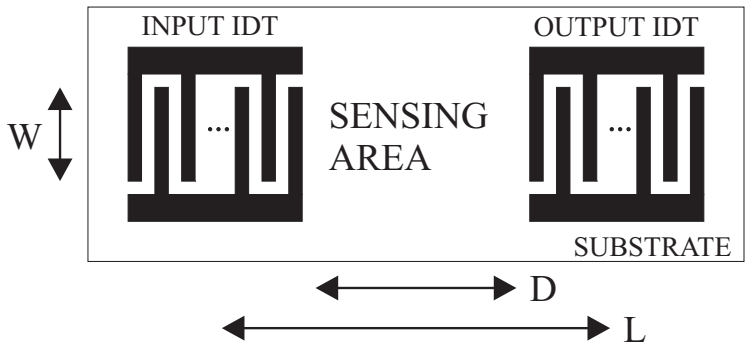

Figure 1. Schematic representation of the surface acoustic wave (SAW) biosensor seen from top. The acoustic signal is generated via interdigital transducers with a mid-distance separation L and with an aperture W corresponding to the overlap length of the interdigitated electodes. The space left between the edges of the transducers is the sensing part with an area $D \times W$.

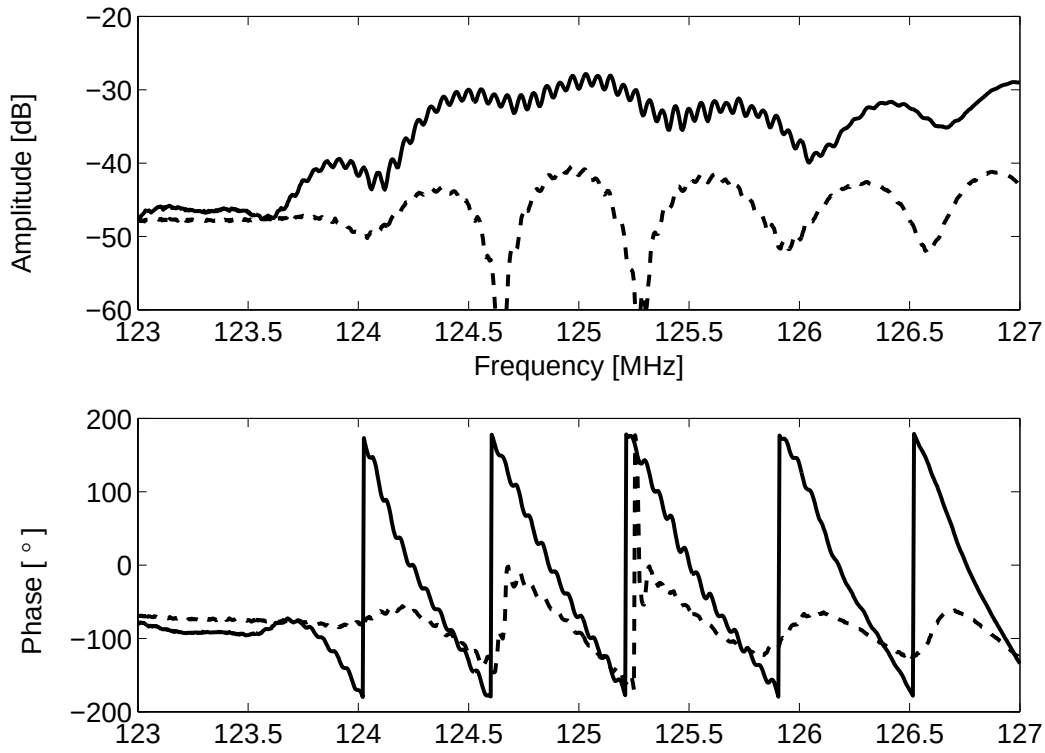

Figure 2. Experimental record of the transfer function of a quartz substrate SAW device showing the effect of water on the transducers. The top graph is the amplitude and the bottom graph is the phase of the electrical signal passing through the acoustic device as a function of the frequency. The solid line is the transfer function in air while the dashed line is the device loaded with water on one or on the two transducers, either partly or totally covering the electrodes of the transducers.

In any cases, the signal attenuation affects the general performance of the sensor from the instrumentation and the sensing aspects. It results in a lack of correlation between surface changes caused by the biomolecules adsorption and the SAW velocity changes measured by phase shifts in the transfer function. Therefore, one desires a method for the efficient shielding of the IDTs against liquids that serves in the same time as liquid holder, namely a *liquid cell*. Examples of liquid cell are reported in the literature.[8–11] Typically, they consist in a pre-molded polydimethylsiloxane (PDMS) cell or in a mechanically drilled Teflon cell that comes in close contact with the device. The cell is mechanically pressed against the surface of the sensor in order to avoid leaks. Despite the flexibility allowed by external liquid cells, these methods miss an integration step at the device processing scale. A liquid cell integrated during the fabrication of SAW biosensors will certainly open and enhance their application. A well designed liquid cell maximizes the sensing surface and minimize interactions with the acoustic wave and with the biochemical species.

In this paper, we address the design and the fabrication of a liquid cell that allows the packaging of SAW biosensors. The liquid cell aims at three characteristics:

- it prevents the presence of liquids on the transducers;
- it has a small disturbance effect on the propagation of the surface acoustic wave;
- it does not interfere with the biochemical sensing event.

2. DESIGN OF THE LIQUID CELL

Our approach is based on the protection of the transducers and of every area out of the acoustic sensing area by a vertical structure above the IDTs. The protecting structure is made of a polymer spacer defined between the sensor surface and a rigid capping layer atop of the spacer. Microfabrication techniques are required for the fabrication of the liquid cell. They allow to reduce the lateral dimensions of polymers that cause acoustic attenuation while in contact with the surface. Therefore, these techniques help to minimize interactions between polymers and the acoustic wave. In addition, they also allow the integration of the packaging at the wafer processing level with reproducible characteristics that address the micron-range scale of the sensor.

Four aspects have been taken in consideration in the design of the liquid cell: (1) the analyte solution must be correctly displayed on the sensing area; (2) the rigid capping layer above the IDTs must not come in contact with the electrodes to avoid a damping of the acoustic wave and their capacitive loading; (3) polymers as spacer cause an acoustic attenuation, consequently these materials must cover the smallest length of the acoustic path on the sensing area; and (4) the sensing area must be kept open for its cleaning prior to any biochemical recognition experiment, for instance with an UV-O_3 cleaning treatment.
Additionally, the packaging is required to withstand the cleaning procedure without contaminating the biochemical solutions. This involves the use of materials presenting good chemical resistance to organic solvents and to UV-O_3 surface treatment.

The SU-8 is a photodefinable epoxy selected to perform the spacer function.[12] Its selection is based on adequate properties:

- photosensitive that allows for a precise patterning of its structure around the IDTs by using standard photolithography techniques;
- high thicknesses attainable (up to 500 μm in one step, much thicker than other photosensitive encapsulant materials like BCB and PMMA) with a high aspect ratio about 1:25;
- stiff epoxy leading to smaller absorption of the acoustic signal than soft polymers;
- good chemical resistance to a wide range of organic solvents and of surface treatments;
- low thermal budget and good adhesion on various materials.

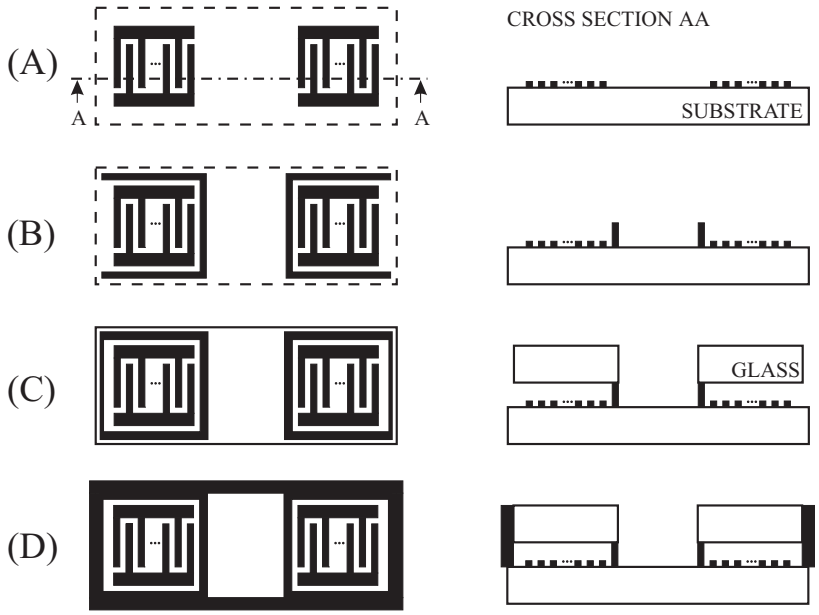

Figure 3. Schematic of the fabrication process. On each drawing, the left side is a top view of the device and the right side is the cross section AA. (A) Initial SAW device is a part of the wafer. (B) SU-8 walls are patterned partly around the transducers and the wafer is diced to release each sensor. (C) The sensor is attached to the printed circuit board and the contact pads are wire bonded to it (step not shown), the top part of the SU-8 walls is manually covered with an epoxy glue, immediately followed by the placement of the quartz glass capping and the curing of the epoxy. (D) The left parts are filled with the same epoxy glue to complete the protection and the packaging of the device. The liquid cell defines a well of precise dimensions above the sensing area of the packaged sensor.

The SU-8 spacer shaped as walls around the IDTs performs a continuous physical separation between the transducers and the sensing area. Because of its position above the acoustic path, this separating wall must be thin to minimize the acoustic damping and wide enough to assure a continuous and rigid physical contact with the sensor. In the present case, a compromise has been found with a 150 μm wide wall. Outside the acoustic path, the walls are larger to increase the adhesion surface between the SU-8 and the sensor on one side, and with the capping layer on the other side.

As capping material, quartz is selected because of its mechanical stiffness, its optical transparency that allows to visually check for the unwanted presence of liquids above the capped transducers, its electrical insulation to avoid interaction with the electromagnetic field emitted by the IDTs, and finally its resistance to a numerous amount of chemical products and surface treatments.

3. FABRICATION OF THE LIQUID CELL

We have used a two steps method to fabricate the liquid cell. The first step is achieved at the wafer level. It consists in the patterning of the SU-8 walls. The second step is achieved at the device level after the dicing of the wafer. It consists in the manual placement of the quartz capping. The fabrication methodology is schematically depicted in Figure 3 and described for a particular example here after. The fabrication method can be extended to various types of substrates and transducers designs without requiring extra developments.

The liquid cell was fabricated on a Love-mode SAW devices made on a 3 inches diameter and 500 μm thick ST-cut (42.5° Y-cut) quartz substrate (China National Scientific Instruments and Materials Corp., Hangzhou, P. R. of China) covered with a 1.2 μm thick silicon dioxide layer obtained by plasma-enhanced chemical vapor deposition (Plasmalab 100 from Oxford Plasma Technology, England). The IDTs have 100 finger pairs each with L=9 mm, W=3.2 mm and D=5 mm. The finger electrodes were made of 200 nm thick sputtered aluminum with

split-finger geometry to minimize ripples in the passband of the device; each finger is 5 μm wide, and equally spaced such that the finger pairs periodicity corresponds to an acoustic wavelength λ of 40 μm.

For the first step, SU-8 walls with a thickness about 120 μm were obtained by using the following recipe. Photosensitive SU-8 type 2075 (Microchem Corp., MA) was spin coated with an acceleration of 100 RPM/s to reach 500 RPM that was held for 10 seconds, and followed by an acceleration of 300 RPM/s to reach 1500 RPM that was held during 30 seconds. After the spinning, the resist was baked for 3 hours at 95°C on a hotplate after a slow temperature ramp up in order to avoid stresses cracks in the epoxy layer. The SU-8 patterns were obtained by soft contact lithography on a Karl-Süss MA6 mask aligner (SUSS MicroTech Inc., VT) for 5 cycles of 10 seconds and a rest time of 60 seconds between each exposure cycle. The exposure was followed by a baking of 15 minutes at 95°C on a hotplate after a slow temperature ramp up to finish the reticulation of the SU-8. The unexposed epoxy was then dissolved in propylene glycol monomethyl ether acetate (PGMEA) with ultrasonication for 10 minutes. Figure 4(a) shows the resulting SU-8 structure patterned around the IDT. Following that step, the wafer was diced to release each sensors with the patterned SU-8 walls. The devices were subsequently wire bonded to a printed circuit board for electrical characterization.

For the second step, quartz glasses of 5 mm by 5 mm and 500 μm thick were placed and glued above the SU-8 structures. An epoxy glue (Epotek H54 from Epoxy Technology, MA, USA) was manually dispensed above the walls and followed by the placement of the glass. The final bonding between the SU-8 walls and the glass was obtained by a 15 minutes curing of the epoxy at 100°C. The flatness of the top surface of SU-8 helped for the perfect sealing between the walls and the capping. The same epoxy glue was used to make a 1 mm wide and 1-2 mm high well around the rest of the device and above the contact pads. This procedure defined an open liquid cell above the acoustic sensing surface with dimensions 4.7 mm ($= D$) by 3.5 mm ($> W$). Figure 4(b) shows a scanning electron microscope (SEM) image of the cross section of the packaged device. The fully packaged SAW biosensor itself is pictured in Figure 4(c).

4. PERFORMANCE AND DISCUSSION

In this section, the performance of the SU-8 liquid cell is evaluated and discussed. For that evaluation, we analyze the acoustic damping due to the liquid cell in a first place and we report a biochemical recognition experiment performed on the packaged SAW biosensor in a second place.

The liquid cell prevents the presence of liquids on the transducers and has a small disturbance effect on the propagation of the acoustic wave. The influence of the SU-8 walls on the acoustic performance of the device is shown in Figure 5 where the amplitude of the transfer function was measured in different situations on an identical device before the capping: with and without the SU-8 walls and with and without water loading. A loss of 7.7 dB is measured at the center frequency f_0=123.2 MHz, caused by the SU-8 walls on the acoustic path between the two transducers. Although designed with a 150 μm width, each wall covers an effective length of 160 μm caused by the aspect ratio of SU-8. Therefore, we estimate the attenuation of the shear acoustic wave by a factor of $\sim$1 dB per acoustic wavelength ($\sim$1 dB/λ). This figure helps to evaluate the influence of the packaging on the acoustic characteristics of the sensor and serves as guideline for the miniaturization of the device. It can also be seen on Figure 5 that the SU-8 provides an efficient shielding against the negative influence of the water loading when it spreads over the entire sensor, including the transducers.

In terms of the critical dimensions to attribute to the walls and to the acoustic wavelength, one is interested in smaller wavelengths to achieve SAW biosensors with higher operating frequencies. The attributed dimensions of the liquid cell is determined by the figure of 1 dB/λ. Different factors are involved in the design of the SU-8 liquid cell for the miniaturization of the device. Because of the precise patterning allowed with the photosensitive epoxy, minimum dimensions are mainly limited by the aspect ratio of the SU-8 and in our case by the manual alignment step of the glass capping that requires a relatively wide top surface. The height of the SU-8 walls must exceed one acoustic wavelength to avoid interactions between the electromagnetic field of the transducers and the capping material. In the present case the SU-8 was three λ high; a carefully addressed investigation of the dimensions of the SU-8 walls would help to determine the impact of the liquid cell geometry on the performance of the SAW biosensor.

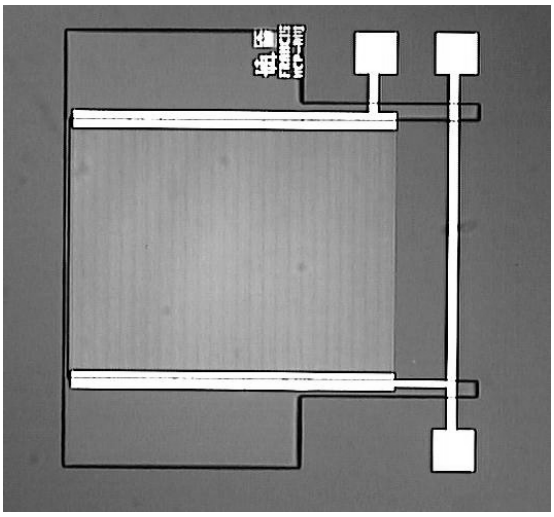

(a)

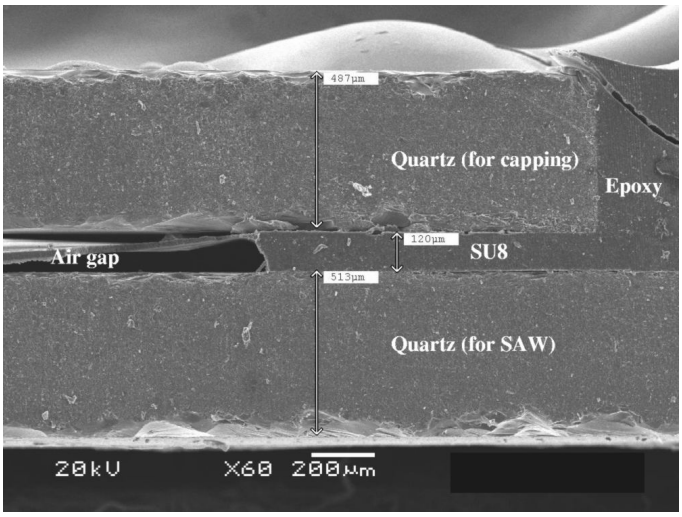

(b)

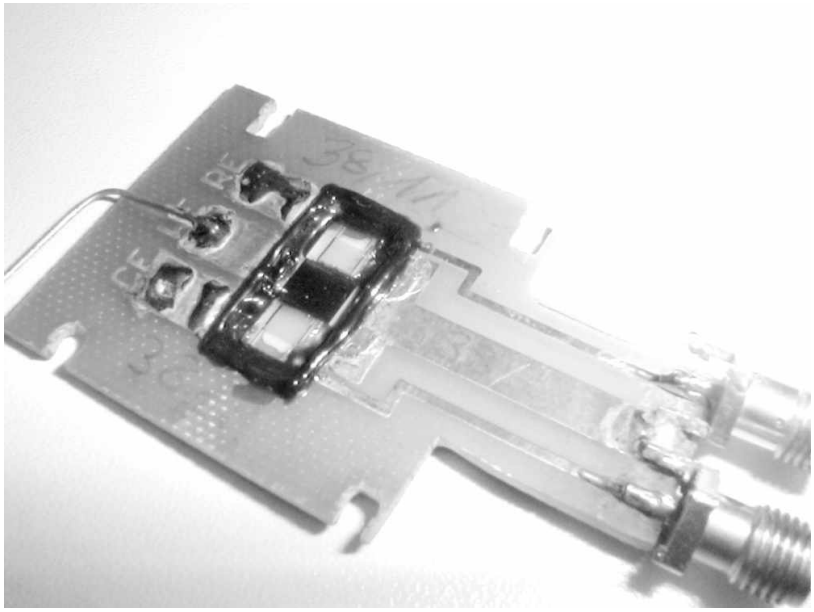

(c)

Figure 4. (a) Optical top view picture of the SU-8 walls patterned around one interdigital transducer. The sensing area is located on the left and is separated from the aluminum electrodes of the transducer by a 150 μm wide on acoustic path, 120 μm high SU-8 wall. (b) A scanning electron microscope (SEM) image of the cross section of the SU-8 walls above the transducers and the quartz capping. (c) The fully packaged SAW biosensor on the printed circuit board.

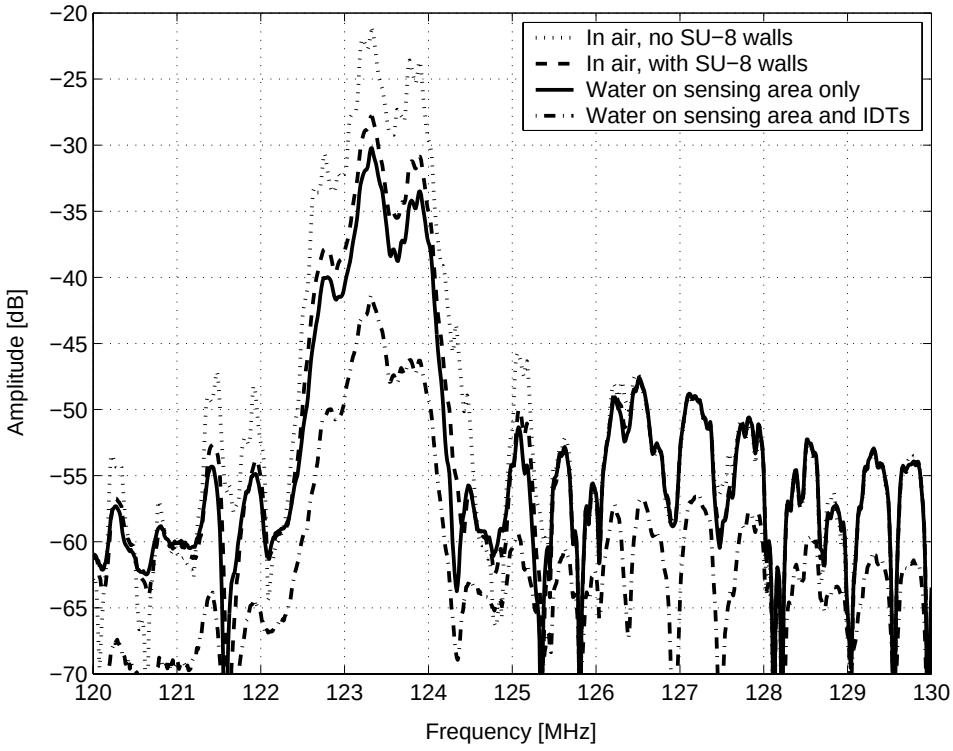

Figure 5. Effect of the SU-8 walls of the liquid cell on the amplitude of the transfer function. The figure displays the amplitude of the electrical signal as a function of the frequency in different situations indicated by the legend (the water loading is in addition to the SU-8 walls).

To illustrate the effectiveness of the SU8 liquid cell, we report the monitoring of protein adsorption by the fully packaged Love-mode SAW biosensor described in section 3. The sensing area was covered by a 50 nm gold layer on a 10 nm titanium adhesion layer to interface the sensor with an hydrophobic self-assembled monolayer (SAM). The device was cleaned for 15 minutes in a UV-O_3 chamber, immediately followed by the coating of the sensing area with a drop of a 1mM stearyl mercaptan (Sigma-Aldrich) solution in ethanol. The deposition of the hydrophobic SAM took place during 3 hours after which the device was rinsed with ethanol and dried with a stream of nitrogen. As protein, type I fibrinogen from human plasma (Sigma-Aldrich) was diluted in PBS buffer (137 mM $NaCl$, 6.44 mM KH_2PO_4, 2.7 mM KCl and 8 mM Na_2HPO_4) to a concentration of 46 μg/ml. The adsorption of the protein on the sensing surface was monitored by the delay phase of the SAW biosensor at the central frequency f_0=123.2 MHz on a HP4396A Network Analyzer (Hewlett-Packard Company, CA). The fibrinogen adsorption was preceded and followed by a rinsing step with PBS buffer and water. Figure 6 reports the monitoring of the sensor as a function of time.

The packaging is not preventing the correct operation of the device and is apparently not interfering with the biochemical experiment. The adsorption of the protein on the sensing area causes a SAW velocity shift that appears as a delay phase shift through the IDTs. The adsorbed protein mass per surface unit Δm is related to the phase difference $\Delta\phi$ (in degrees) between starting and stopping points of the experience by[3]

$$\Delta m = \frac{\lambda \times \Delta\phi}{360 \times D \times S} \tag{1}$$

where D=4.7 mm is the effective sensing length, λ=40 μm and S the mass sensitivity of this specific Love-mode SAW biosensor. The mass sensitivity has been calibrated to a value of 280 cm^2/g via copper electrodeposition.[13]

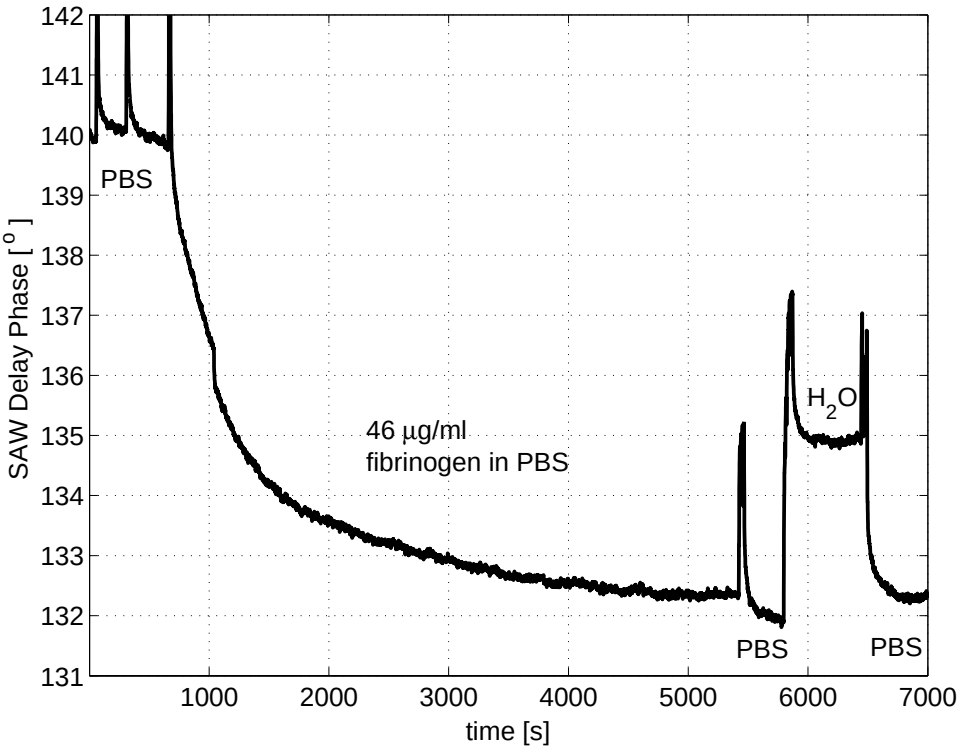

Figure 6. Biorecognition fibrinogen experiment that shows no interference because of the presence of the liquid cell. The delay phase of a Love-mode SAW biosensor is monitored as a function of time. The fibrinogen adsorption on the sensing surface modifies the SAW velocity. This change appears as a delay phase shift because of the electrical transduction.

In the present case, the observed phase shift of 8° in Figure 6 corresponds to a surface density of 675 ng/cm^2 that is a likely value for fibrinogen surface coverage. Based on this observation, we conclude to the absence of interaction between the liquid cell and the sensing aspect.

A detailed comparison of our approach with other types of liquid cell is difficult to give because of a lack of data and studies with regards to its influence on the general performance of the SAW biosensor and partly because of the innovative aspect of the SU-8 liquid cell. One of the most difficult aspect related to a pre-molded liquid cell is the necessity to manually adjust its position above the sensing surface and to mechanically press the cell against the SAW device till a perfect sealing is reached so that no leaks can occur during the whole biochemical experiment. The position of the cell and the pressure are inevitably varying from experiments to experiments and may result in a lack of experimental reproducibility. In comparison, we claim that the precise patterning of the SU-8 associated to the rigidity and the stability of our whole packaging solution is an improvement that assures the experimental reproducibility of SAW biosensors.

5. CONCLUSION AND FUTURE DEVELOPMENTS

The packaging of surface acoustic wave biosensors is solved by the realization of a SU-8 based liquid cell. We have shown that the SU-8 assures the sealing of a capping layer above the transducers and prevents liquids to contact the electrodes of the transducers. The design of the liquid cell results in an attenuation factor about 1 dB per acoustic wavelength of SU-8 on the acoustic sensing path. The materials selected for the fabrication of the liquid cell have a good chemical resistance and are apparently not interfering with the biochemical sensing event. The presented SU-8 liquid cell is a basic step in the integration of the packaging of SAW biosensors at the wafer processing level but the influence of design parameters on the instrumentation and the sensing characteristics of the SAW biosensor is part of future developments.

For future developments, improvements are required to increase the integration of IC fabrication techniques in the realization of the packaging solution. A first improvement to the presented solution resides in a microfluidic system for liquid flow above the sensing surface, an aspect that is missing in the developed liquid cell and although a static fluid display does not prevent the correct operation of the biosensor. An hybrid approach is based on the advantage provided by the SU-8 walls in term of integration, low acoustic attenuation and reproducibility, and by the flexibility of a pre-molded external cell. The SU-8 plays the role of a microfabricated O-ring precisely defining the sensing area; above this O-ring, the glass capping could be advantageously replaced by a removable PDMS molded microfluidic. This solution has the disadvantage of requiring a mechanical set-up to apply a pressure for the sealing of the SU-8/PDMS interface.

A second improvement at the wafer level is the wafer bonding of the capping. The identification of two steps in the fabrication methodology let appear a clear break between batch and manual processes in the packaging of the SAW biosensor. The wafer bonding of a full glass wafer requires a glass with holed structures above the sensing area, for instance with sand blasted openings. The advantage is that SU-8 can be used as bonding material. This solution is an opportunity to have a full batch processing of the packaging, unless other packaging methods are developed.

APPENDIX A. ELECTRICAL MODEL OF THE SAW DEVICE

Surface acoustic wave devices and interdigital transducers have been described abundantly in the literature.[14, 15] We use the electrical model to evaluate the effect a liquid loading on the electrical instrumentation of the device. The ideal transducer is modeled by a radiation conductance $G_a(f)$ that is function of the frequency f connected in parallel with a static capacitance C_T. The electrical admittance of the transducer is written as

$$Y_{IDT}(f) = G_a(f) + j2\pi f C_T \tag{2}$$

and an expression for C_T is NWC_0, where N is the number of finger pairs with an acoustic aperture W corresponding to the overlap length of the fingers and C_0 the capacitance per finger pair and per unit length. The *synchronous frequency* f_0 is the ratio between the acoustic velocity V and the finger pairs periodicity λ (i.e. $f_0 = V/\lambda$). For frequencies near the synchronous frequency, the radiation conductance is approximated by

$$G_a(f) \simeq 8K^2 f_0 N^2 W C_0 \left(\frac{\sin x}{x}\right)^2, \tag{3}$$

where $x = N\pi(f - f_0)/f_0$ and K^2 is the electromechanical coupling constant of the piezoelectric substrate. The transfer function $H(f)$ of a lossless SAW delay line relates the output (or load) voltage V_L to the source voltage V_S and is given by

$$H(f) = \frac{V_L}{V_S} = \frac{Y_{DL}R}{(1 + Y_{IDT}R)^2 - (Y_{DL}R)^2} \tag{4}$$

where R is the source and load impedances supposed identical and equal to 50 Ohms, and Y_{DL} is a transfer admittance given by

$$Y_{DL} = G_a(f) \exp\left\{j\left(\pi - 2x - 2\pi f L/V\right)\right\}. \tag{5}$$

The electrical model of the SAW device allows us to evaluate the effect of water loading on the transducers. In a rough estimation, the capacitance per finger pair and per unit length is given by $C_0 = (\varepsilon_{rS} + \varepsilon_{rL}) \times \varepsilon_0$, where ε_0 is the vacuum permittivity (8.854 pF/m), ε_r is the relative permittivity and the subscripts S and L refer to the substrate and the loading, respectively. We compare the effect of water loading ($\varepsilon_r = 80$) of the transducers for two classical substrates with low and high K^2: quartz and lithium niobate (LNO). The maximum amplitude of the transfer function, that is $20 \log \|H(f)\|$, is simulated as a function of the value of C_0. The parameters of the simulation are given in Table 1 and with $W = 3.2$ mm, $L = 9$ mm and $\lambda = 40$ μm.

Figure 7 displays the net change of the amplitude with air and with water above the electrodes of the transducers. The attenuation is more pronounced on the quartz with a loss about 12 dB, while for LNO the loss is lower with a value of 6.9 dB. This difference is mainly due to the high value of both the dielectric permittivity and the electromechanical coupling constant of LNO.

	Quartz	LNO
K^2	0.0011	0.046
f_0	126.5 MHz	87.2 MHz
V	5060 m/s	3488 m/s
N	100	40

Table 1. Simulation parameters

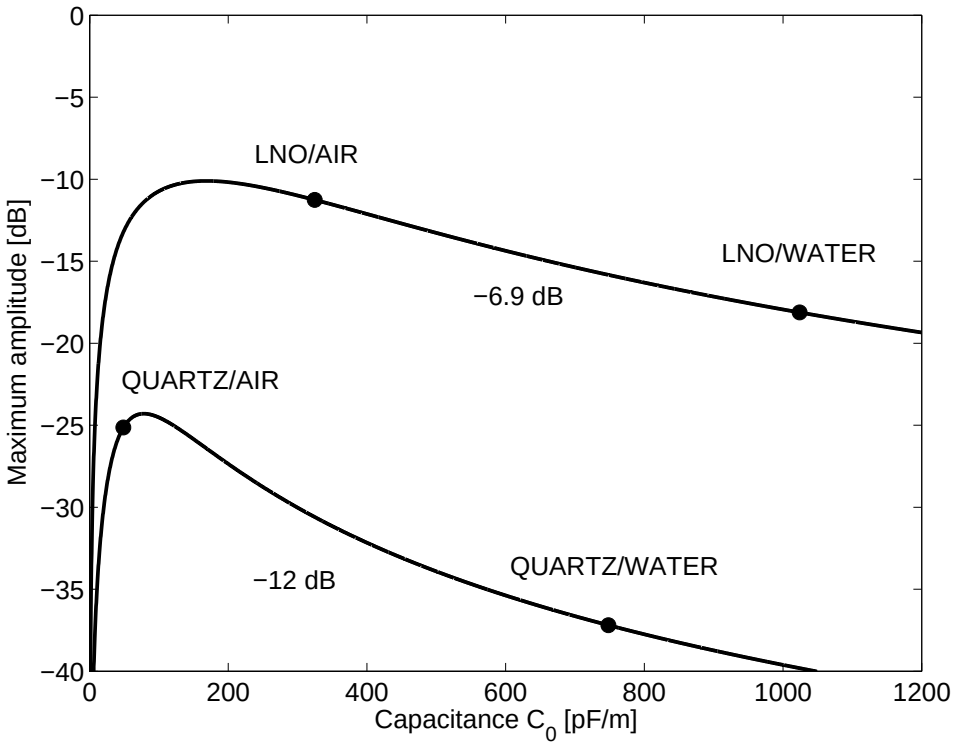

Figure 7. Theoretical evolution of the maximum electrical amplitude of the SAW device as a function of the capacitance per finger pair and per unit length (C_0) for lithium niobate (LNO, upper curve) and quartz (lower curve). The dots are the values corresponding to air and water above the finger electrodes.

ACKNOWLEDGMENTS

L. A. Francis thanks the FRIA (Fonds pour la Formation à la Recherche dans l'Industrie et dans l'Agriculture) for financial support.

REFERENCES

1. D. S. Ballantine, R. M. White, S. J. Martin, M. J. Ricco, E. T. Zellers, G. C. Frye, and H. Wohltjen, *Acoustic wave sensors. Theory, design, and physico-chemical applications*, Academic Press, San Diego, 1997.
2. A. Leidl, I. Oberlack, U. Schaber, B. Mader, and S. Drost, "Surface acoustic wave device and applications in liquid sensing," *Smart Mater. Struct.* **6**, pp. 680–688, 1997.
3. B. Jakoby and M. J. Vellekoop, "Properties of Love waves: applications in sensors," *Smart Matr. Struct.* **6**, pp. 668–679, 1997.
4. R. L. Baer, C. A. Flory, M. Tom-Moy, and D. S. Solomon, "STW chemical sensors," in *IEEE Trans. Ultrasonics Symp.*, pp. 293–298, 1992.
5. G. L. Harding, J. Du, P. R. Pencher, D. Barnett, and E. Howe, "Love wave acoustic immunosensor operating in liquid," *Sensors and Actuators A* **61**, pp. 279–286, 1997.
6. R. M. White and F. W. Voltmer, "Direct piezoelectric coupling to surface elastic waves," *App. Phys. Lett.* **7**, pp. 314–316, 1965.
7. B. Jakoby and M. J. Vellekoop, "Analysis and optimization of Love wave liquid sensors," in *IEEE Trans. on UFFC*, pp. 1293–1302, 1998.
8. E. Gizeli, A. C. Stevenson, N. J. Goddard, and C. R. Lowe, "A novel love-plate acoustic sensor utilizing polymer overlayers," in *IEEE Trans. on UFFC*, pp. 657–659, 1992.
9. O. Tamarin, C. Déjous, D. Rebière, J. Pistré, S. Comeau, D. Moynet, and J. Bezian, "Study of acoustic Love wave devices for real time bacteriophage detection," *Sensors and Actuators B* **91**, pp. 275–284, 2003.
10. E. Gizeli, F.Bender, A. Rasmusson, K. Saha, F. Josse, and R. Cernosek, "Sensitivity of the acoustic waveguide biosensor to protein binding as a function of the waveguide properties," *Biosensors and Bioelectronics* **18**, pp. 1399–1406, 2003.
11. D. W. Branch and S. M. Brozik, "Low-level detection of a bacillus anthracis simulant using Love-wave biosensors on 36°YX $LiTaO_3$," *Biosensors and Bioelectronics* **19**, pp. 849–859, 2004.
12. R. J. Jackman, T. M. Floyd, R. Ghodssi, M. A. Schmidt, and K. F. Jensen, "Microfluidic systems with on-line UV detection fabricated in photodefinable epoxy," *J. Micromech. and Microeng.* **11**, pp. 263–269, 2001.
13. J.-M. Friedt, L. Francis, K.-H. Choi, F. Frederix, and A. Campitelli, "Combined atomic force microscope and acoustic wave devices: Application to electrodeposition," *J. Vac. Sci. Technol. A* **21**, pp. 1500–1505, 2003.
14. C. Campbell, *Surface acoustic wave devices and their signal processing applications*, Academic Press, San Diego, 1989.
15. D. Royer and E. Dieulesaint, *Ondes élastiques dans les solides*, vol. 2, Masson, Paris, 1999.